Journal of the Korean Physical Society, Vol. 67, No. 2, July 2015, pp. 366∼370

Synthesis of ZnS Films on Si(100) Wafers by Using Chemical Bath Deposition Assisted by the Complexing Agent Ethylenediamine

He-Jie Zhu
Key Lab of Material Physics of Ministry of Education, School of Physics and Engineering, Zhengzhou University, Zhengzhou 450052, China

Xue-Mei Wang
College of Information Science and Engineering, Henan University of Technology, Zhengzhou 450001, China

Xiao-Yong Gao*
School of Physics and Engineering, Zhengzhou University, Zhengzhou 450052, China

(Received 15 April 2015, in final form 1 June 2015)

Low-cost synthesis of high-quality ZnS films on silicon wafers is of much importance to the ZnS-based heterojunction blue light-emitting device integrated with silicon. Thus, a series of ZnS films were chemically synthesized at low cost on Si(100) wafers at 353 K under a mixed acidic solution with a pH of 4 with zinc acetate and thioacetamide as precursors and with ethylenediamine and hydrochloric acid as the complexing agent and the pH value modifier, respectively. The effects of the ethylenediamine concentration on the crystallization, surface morphology, and optical properties of the ZnS films were investigated by using X-ray diffractometry, scanning electron microscopy, spectrophotometry, and fluorescence spectroscopy. A mechanism for the formation of ZnS film under an acidic condition was also proposed. All of the ZnS films were polycrystalline in nature, with a dominant cubic phase and a small amounts of hexagonal phases. The crystallization and the surface pattern of the films were clearly improved with increasing ethylenediamine concentration due to its enhanced complexing role. The absorption edge of the films almost underwent a blue shift with increasing ethylenediamine concentration, which was largely attributed to the quantum confinement effects caused by the small particle size of the polycrystalline ZnS films. Defect species and the corresponding strengths of the ZnS films were strongly affected by the ethylenediamine concentration.

PACS numbers: 78.66.Hf, 78.40.Fy, 61.10.Nz
Keywords: Chemical bath deposition, ZnS films, Ethylenediamine concentration, Optical properties
DOI: 10.3938/jkps.67.366

I. INTRODUCTION

Zinc sulfide (ZnS) is an important II-VI compound semiconductor with excellent physical properties. The compound has been extensively investigated because of its wide band gap in the range between 3.6 and 3.8 eV and high refractive index of 2.3. ZnS is widely used in optoelectronics such as blue light-emitting devices [1], electroluminescence devices, photovoltaic cells, displays [2,3], sensors, and lasers [4]. ZnS nanoparticles are deposited using a variety of techniques such as electrodeposition [5], molecular beam epitaxy [6], chemical vapor deposition [7], magnetron sputtering [8], vacuum evaporation [9,10], and chemical bath deposition (CBD) [11]. Low-cost synthesis of high-quality ZnS film is still of much importance to the ZnS-based heterojunction blue light-emitting device due to its further wide application. In recent years, the CBD method has received more attention because of its many advantages: low cost, easy operation, large freedom of the chosen dopants, and its being free of the harmful problems in high-temperature processes. However, CBD alone also exhibits many disadvantages such as the relatively poor film quality, etc. The utility of the CBD method to synthesis ZnS film is sensitive to the precursor concentration, the complexing agent and especially to the solution's pH value. ZnO, rather than the desired ZnS, is easy to synthesize in strong alkaline solutions due to the hydrolysis of ZnS under strong alkaline conditions. Thus ZnS should be synthesized under appropriate acidic condition. Besides, for the synthesis of high-quality ZnS, the choice of a suitable complexing agent that is soluble in an acidic solution is

*E-mail: xygao@zzu.edu.cn; Tel: +86-371-67767803

of great importance. For ZnS-based blue light-emitting devices, compatibility with traditional silicon integration processing and low cost are keys to their wide application. Although the deposition of ZnS on many substrates by using a variety of means has been reported elsewhere, and the structural, optical and electrical properties of the ZnS have been intensively studied, a study of the synthesis of ZnS on a heavily-doped p-type silicon substrate by using the low-cost CBD method is still valuable for ZnS/Si heterojunction blue light-emitting devices in which heavily p-type silicon is used as a p-type layer. The role soluble ethylenediamine (En) plays as a complexing agent in an acidic solution and the effect of the En concentration on the structural and the optical properties of the ZnS have not been systematically studied so far.

In this study, polycrystalline ZnS films composed of regular nanoparticles were deposited on heavily-doped p-Si(100) substrates by using the CBD in an acidic solution with a pH of 4 that had been confirmed to be the best for the synthesis of high-quality ZnS in our previous work; here, En was used as a complexing agent, and thioacetamide (CH_3CSNH_2,TAA)and zinc acetate as the sulfide source and the zinc source, respectively. The effects of varying the En concentration from 0.00 M to 1.50 M on the microstructure, composition, and optical properties of the resultant ZnS films were determined. A mechanism for the formation of the ZnS film in an acidic solution is also proposed.

II. EXPERIMENTALS

ZnS films composed of regular nanoparticles were deposited on heavily-doped p-Si(100) substrates by using CBD in an acidic mixed solution with zinc acetate, TAA, and En at 353 K. En was used as a complexing agent, and zinc acetate and TAA were used as precursor reactants. Zinc acetate dehydrate (1.00 M), TAA (0.50 M), hydrochloric acid solution (2.00 M), and different concentrations of En solutions were prepared prior to ZnS film deposition. Approximately 10 ml of zinc acetate solution and 10 ml of the En solutions were mixed in a beaker and stirred for several minutes to obtain a homogeneous, milky white emulsion because of the formation of $[Zn(En)]^{2+}$. Exactly 1 ml of hydrochloric acid solution and 40 ml of TAA were added to this white emulsion, and the mixture was stirred for several minutes. The pH of the mixture was adjusted to 4 by adding the hydrochloric acid solution.

Heavily-doped p-type Si(100) substrates were cleaned by using conventional RCA processing. The Si substrates were then placed in mixed solutions that had been previously heated to 353 K in a baker oven and allowed to react at 353 K for 6.5 h. After deposition, the Si substrates coated with ZnS films were removed from the reaction bath, rinsed, ultrasonically rinsed with deionized water, and then naturally dried.

The complexing agent has an important function in the chemical bath reaction. In this work, En was used as the complexing agent to slow down the release of Zn^{2+} that reacts with the S^{2-} released from TAA to form ZnS. The main chemical reactions involved in the acidic solution can be described as follows [12]:

$$Zn^{2+} + En \rightleftharpoons [Zn(En)]^{2+}, \quad (1)$$

$$CH_3CSNH_2 + H^+ \rightarrow CH_3 - C \equiv NH^+ + H_2S, \quad (2)$$

$$H_2S + H_2O \rightleftharpoons HS^- + H_3O^+, \quad (3)$$

$$HS^- + H_2O \rightleftharpoons S^{2-} + H^+, \quad (4)$$

$$Zn^{2+} + S^{2-} \rightarrow ZnS + En. \quad (5)$$

Zn^{2+} from zinc acetate prefers to react with the complexing agent (En) to form a $[Zn(En)]^{2+}$ complex rather than directly reacting with S^{2-} to form ZnS. $[Zn(En)]^{2+}$ is then adsorbed by the substrate and reacts directly with S^{2-} to form ZnS. The release of free Zn^{2+} from $[Zn(En)]^{2+}$ is comparably slower than that of the S^{2-}.

X-ray diffraction (XRD) patterns were obtained by using an automated X'pert Philips instrument with CuKα radiation. The surface morphologies of the films were recorded by using a field-emission scanning electron microscope (FE-SEM, JSM-6060). The optical absorption and photoluminescence spectra of the films were obtained by using a UV-VIS spectrometer (Shimadzu UV-3150) and a fluorescent spectrometer (FluoroMax-4), respectively. All measurements were conducted at room temperature.

III. RESULTS AND DISCUSSION

1. Structural Properties

In general, ZnS crystallizes in a cubic zinc-blende or hexagonal wurtzite form. The cubic structure is stable at room temperature whereas the hexagonal structure is stable at high temperatures [13]. Figure 1 shows the XRD patterns of ZnS films synthesized with En concentrations ranging from 0.00 M to 1.50 M. The XRD patterns show the polycrystalline characteristics of the ZnS films. Figure 1(b) shows strong (111), (220), and (311) diffraction peaks, which are attributed to the crystal face diffractions of the cubic ZnS phase (Card No. 01-080-0020) in the ZnS film deposited without En. At En concentration = 0.50 M, the characteristic diffraction peaks of the cubic ZnS phase disappear; however, further increases in En concentration produce the characteristic

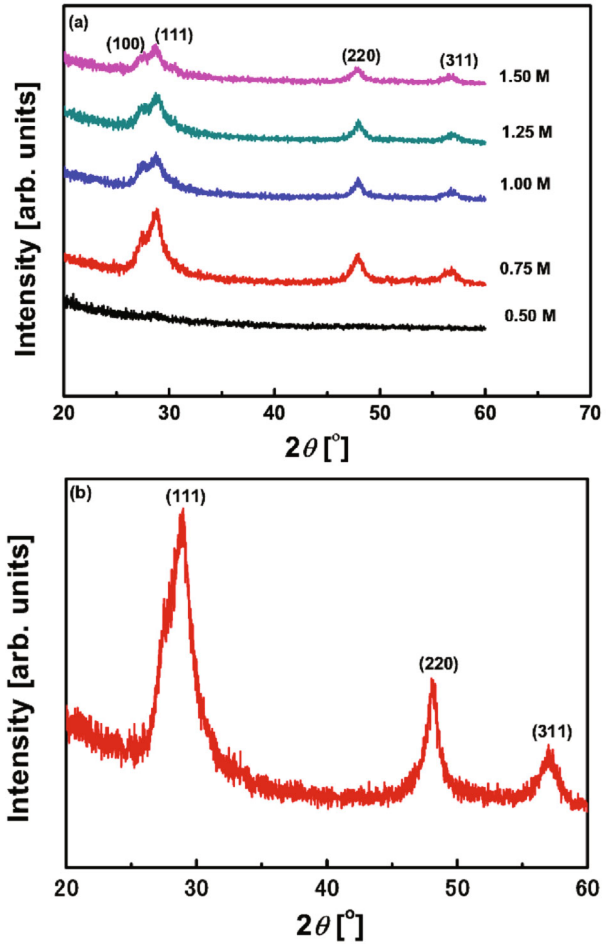

Fig. 1. (Color online) XRD patterns of the ZnS films with En concentrations (a) ranging from 0.50 to 1.50 M and (b) of 0.00 M.

peaks of the cubic ZnS phase once more. Thus, some organic substances (maybe $[Zn(En)]^{2+}$) are probably absorbed onto the ZnS particles and shield the structural information from ZnS particles at an En concentration of 0.50 M. A weak (100) diffraction peak of the hexagonal ZnS phase (Card No. 00-003-1093) begins to appear when the En concentration exceeds 0.50 M. Thus, a small amount of the hexagonal ZnS phase coexists with the cubic ZnS phase. This has not been reported in the literature so far.

The average crystallite sizes of the ZnS films can be determined from the XRD pattern according to Scherrer's equation [14]:

$$D = 0.9\lambda/(\beta\cos\theta), \tag{6}$$

where D is the average crystallite size, λ is the X-ray wavelength ($\lambda = 0.15406$ nm), θ is the Bragg angle, and β is the full width at half maximum. The average crystallite sizes along the <111> and the <220> orientations of the ZnS films synthesized by using different En concentrations are given in Table 1. The average crystallite

Table 1. Average crystallite sizes along the <111> and the <220> orientations for the ZnS films synthesized by using different En concentrations.

En conc. [M]	Crystal orientation	D [nm]
0.00	<111>	13.0
	<220>	25.0
0.75	<111>	11.5
	<220>	21.5
1.00	<111>	23.0
	<220>	30.0
1.25	<111>	11.5
	<220>	18.0
1.50	<111>	14.5
	<220>	21.5

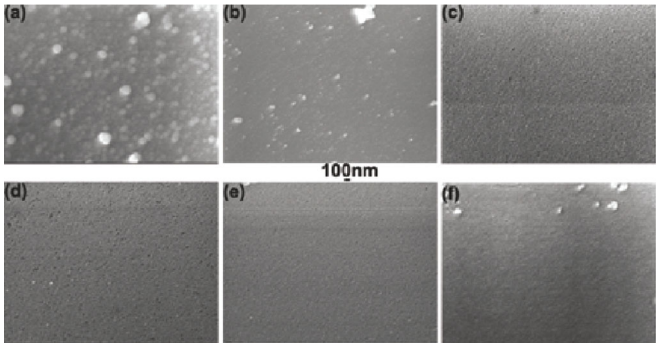

Fig. 2. Surface morphologies of the ZnS films synthesized by using En concentration of (a) 0.00 M, (b) 0.50 M, (c) 0.75 M, (d) 1.00 M, (e) 1.25 M, and (f) 1.50 M.

sizes along the <111> orientation roughly vary from 11.5 to 14.5 nm, and those along the <220> orientation from 18.0 to 25.0 nm, except for the film synthesized with En concentration of 1.00 M.

Figure 2 shows the surface morphologies of the ZnS films synthesized by using different En concentrations. The ZnS films show uniform morphologies and adhere well onto the Si substrates. As the En concentration is increased from 0.50 M to 1.25 M, the film's surface becomes smoother and more compact; continuous uniformity and the absence of agglomerated particles are also observed. The ZnS film consists of small, densely-packed ZnS particles without pinholes, which indicates homogeneity. However, this morphology changes when the En concentration is 1.00 M, which may be due to the poor reproducibility of CBD. The film deposited without En shows a hemispherical structure composed of agglomerated particles (approximately 90 nm). The densely - packed nature and the non-uniformity of the film are due to the rapid release of Zn^{2+} and their reaction with S^{2-}, which agrees well with our XRD results.

Table 2. The calculated band gaps of the ZnS films synthesized by using different En concentrations in terms of the Tauc equation.

En conc. [M]	0.00	0.50	0.75	1.00	1.25	1.50
E_{opt} [eV]	3.35	3.40	3.64	3.38	3.73	3.75

2. Optical Properties

The optical band gap of a semiconductor material can be obtained by linear fitting of the Tauc curve [15]:

$$\alpha \propto (h\nu - E_{opt})^n, \tag{7}$$

where α is the absorption coefficient, hν is the photon energy, and E_{opt} is the optical bandgap. The index n characterizes the transition between the valence and the conduction bands. For a direct bandgap semiconductor, n is 1/2. By plotting $\alpha^2(h\nu)$, the bandgap values of the films can be estimated from the initial absorption edge line when $\alpha = 0$. Figure 3 shows the $\alpha^2(h\nu)$ plot of the ZnS film synthesized by using an En concentration of 0.00 M. The inset shows the corresponding absorbance spectrum of the film. The optical band gap of the film is 3.35 eV (the corresponding absorption edge at 370 nm). The band gaps of other samples calculated in terms of the Tauc equation are listed in Table 2. The band gaps of the ZnS films are roughly smaller and larger than the typical value for bulk ZnS (3.6 eV) at En concentrations $\leq$ 0.50 M and $>$ 0.50 M, respectively. The band gap of 3.38 eV for the film synthesized with an En concentration of 1.00 M is the only exception. The absorption edge almost performs a blue shift with increasing En concentration. The blue shift of the absorption edge can be attributed to the quantum confinement effects caused by the small particle size of the polycrystalline ZnS films. Similar behaviors were previously reported by Sartale *et al.* [16].

Figure 4 shows the photoluminescence spectra of the ZnS films synthesized by using different En concentrations; here, the excitation wavelength is 310 nm. The photoluminescence spectra of the films indicate a wide light-emitting band in the visible region. The photoluminescence intensity of the light-emitting band shows a close relationship with En concentration. When the En concentration ranges from 0.75 M to 1.50 M, the photoluminescence peak's center in the visible region undergoes a blue shift. In the ZnS films without En or with an En concentration of 0.50 M, the light-emitting band approximately centered between 430 and 450 nm is associated with sulfur vacancies [17, 18], whereas the wide light-emitting band centered at about 470 nm is attributed to existing point defects, *i.e.*, void traps and Zn voids caused by a S deficiency on the film's surface [19, 20]. The shifting of the light-emitting center when the En concentration is initially increased to 0.50 M may be explained by the small amount of Zn^{2+} reacting with

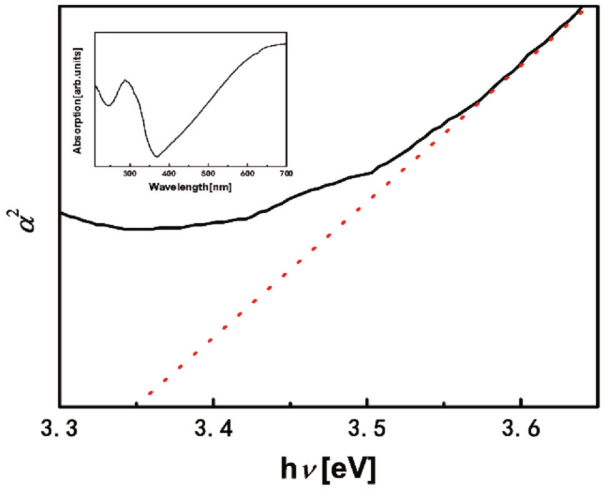

Fig. 3. (Color online) $\alpha^2(h\nu)$ plot of the ZnS film synthesized by using an En concentration of 0.00 M. The inset denotes the corresponding absorption spectrum.

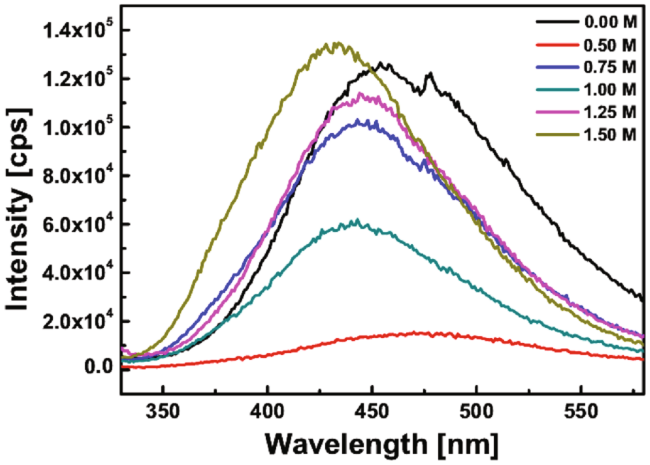

Fig. 4. (Color online) Photoluminescence spectra of the ZnS films synthesized by using different En concentrations.

En (Eq. 1) to form $[Zn(En)]^{2+}$ and release Zn^{2+}. At the same time, free Zn^{2+} reacts directly with free S^{2-} to form ZnS. Compared with free S^{2-}, free Zn^{2+} is insufficient in the deposition solution because of the existing $[Zn(En)]^{2+}$; this insufficiency produces Zn vacancies in the ZnS film. As the En concentration is increased from 0.75 M to 1.50 M, most or all of the Zn^{2+} preferably react with En to form $[Zn(En)]^{2+}$. Although $[Zn(En)]^{2+}$ releases Zn^{2+} very slowly and decelerates the formation of ZnS, the Zn^{2+} released from $[Zn(En)]^{2+}$ is relatively greater in amount than free S^{2-}; thus, sulfur vacancies are produced. Defect species (*i.e.*, zinc and sulfur vacancies) and the corresponding strength of the ZnS films are affected by the En concentration. As the En concentration is increased, defect species change from zinc vacancies to sulfur vacancies. The zinc vacancy's strength gradually decreases with a gradual increase in the sul-

fur vacancy's strength; these findings are confirmed by the shift in the light-emitting center and the change in photoluminescence strength observed in the films.

IV. CONCLUSION

Nanocrystalline ZnS films deposited on heavily-doped *p*-type Si(100) substrates were obtained by using CBD with different En concentrations. The ZnS films are mainly composed of cubic ZnS phases and small amounts of the hexagonal ZnS phases. As the En concentration is increased from 0.50 M to 1.25 M, the film's surface becomes increasingly smooth and compact, showing continuous uniformity and the absence of agglomerated particles. The absorption edge of the films almost performs a blue shift with increasing En concentration. The blue shift of the absorption edge can be attributed to the quantum confinement effects caused by the small particle size of the polycrystalline ZnS films. All of the films show a wide light-emitting band. As the En concentration is increased, defect species in the films change from zinc vacancies to sulfur vacancies. Zinc vacancy's strength gradually decreases with a gradual increase in the sulfur vacancy's strength. These findings may be confirmed by the shift in the light-emitting center and the change in photoluminescence strength observed in the films.

ACKNOWLEDGMENTS

The authors would like to gratefully acknowledge support by the National Science Foundation of China (grant No.60807001) and the Foundation of Young Key Teachers from University of Henan Province (grant No. 2011GGJS-008).

REFERENCES

[1] S. Coe, W. K. Woo, M. Bawendi and V. Bulovic, Nature **420**, 800 (2002).
[2] M. C. Beard, G. M. Turner and C. A. Schmuttenmaer, Nano Lett. **2**, 983 (2002).
[3] R. P. Raffaelle, S. L. Castro, A. F. Hepp and S. G. Bailey, Prog. Photovoltaics **10**, 433 (2002).
[4] V. I. Klimov, A. A. Mikhailovsky, S. Xu, A. Malko, J. A. Hollingsworth, C. A. Leatherdale, H. J. Eisler and M. G. Bawendi, Science **290**, 314 (2000).
[5] D. Gal, G. Hodes, D. Lincot and H. W. Schock, Thin Solid Films **361-362**, 79 (2000).
[6] Y. Kavanagh and D. C. Cameron, Thin Solid Films **398-399**, 24 (2001).
[7] D. Barreca, A. Gasparotto, C. Maragno, E. Tondello and C. Sada, Chem. Vapour Depos. **10**, 229 (2004).
[8] H. Murray and A. Tosser, Thin Solid Films **24**, 165 (1974).
[9] X. H. Cheng, Z. R. Song and Y. H. Yu, Rare Metal Mater. Eng. **35**, 1192 (2006).
[10] L. X. Rong, Q. Li, R. P. Li, C. Z. Zhang, H. Q. Cong and X. Q. Song, Acta Scientiarum Naturalium Universitatis Neimongol. **30**, 454 (1999)(in Chinese).
[11] P. O'Brien and J. McAleese, Mater. Chem. **8**, 2309 (1998).
[12] K. Y. Rajpure, A. L. Dhebe, C. D. Lokhande and C. H. Bhosale, Mater. Chem. Phys. **56**, 177 (1998).
[13] L. I. Berger, *Semiconductor Materials* (CRC, Boca Raton, 1997), p. 86.
[14] Y. J. Hsiao, C. W. Liu, B. T. Dai and Y. H. Chang, J. Alloys Compd. **475**, 698 (2009).
[15] J. Tauc, *Amorphous and Liquid Semiconductor* (Plenum, New York, 1974), p. 159.
[16] S. D. Sartale, B. R. Sankapal, M. Lux-Steiner and A. Ennaoui, Thin Solid Films **480-481**, 168 (2005).
[17] B. Bodo and P. Kalita, in Proc. AIP, Conf, Proc. **1276**, 3 (2010).
[18] H. Y. Lu and S. Y. Chu, J. Crystal Growth **265**, 476 (2004) (in Chinese).
[19] R. N. Bhargava and D. Gallagher, Phys. Rev. Lett. **72**, 416 (1994).
[20] M. Godlewski and M. Skowronski, Phys. Rev. B **32**, 4007 (1985).